

Article

Structure from Motion Photogrammetry as an Effective Nondestructive Technique to Monitor Morphological Plasticity in Benthic Organisms: The Case Study of *Sarcotragus foetidus* Schmidt, 1862 (Porifera, Demospongiae) in the Portofino MPA

Torcuato Pulido Mantas ^{1,2}, Camilla Roveta ^{1,2,*}, Barbara Calcinai ^{1,2}, Fabio Benelli ¹, Martina Coppari ^{1,2}, Cristina Gioia Di Camillo ^{1,2}, Ubaldo Pantaleo ³, Stefania Puce ¹ and Carlo Cerrano ^{1,2,4,5}

- ¹ Department of Life and Environmental Sciences, Università Politecnica delle Marche, Via Brecce Bianche s.n.c., 60131 Ancona, Italy; t.pulido@staff.univpm.it (T.P.M.); b.calcinai@staff.univpm.it (B.C.); fabiobenelli.bio@gmail.com (F.B.); m.coppari@staff.univpm.it (M.C.); c.dicamillo@staff.univpm.it (C.G.D.C.); s.puce@staff.univpm.it (S.P.); c.cerrano@staff.univpm.it (C.C.)
- ² National Biodiversity Future Center (NBFC), Piazza Marina 61, 90133 Palermo, Italy
- ³ Underwater Bio-Cartography (UBICA) S.r.l., Via San Siro 6, 16124 Genova, Italy; ubaldo_pantaleo@hotmail.it
- ⁴ Department of Integrative Marine Ecology, Stazione Zoologica Anton Dohrn, Via Francesco Caracciolo, 80122 Naples, Italy
- ⁵ Fano Marine Center, Viale Adriatico 1, 61032 Fano, Italy
- * Correspondence: c.roveta@staff.univpm.it

Abstract: Porifera are essential components of marine ecosystems, providing valuable ecological functions. Traditional approaches to estimating sponge growth and biomass are destructive and often not suitable for certain morphologies. The implementation of new innovative techniques and nondestructive methodologies have allowed for a more sustainable approach. In this study, a population of *Sarcotragus foetidus* Schmidt, 1862 (Demospongiae, Dictyoceratida, Irciniidae), thriving inside the Portofino Marine Protected Area, was monitored using Structure from Motion photogrammetry over a period of 6 years, from September 2017 to October 2023. Of the 20 initial individuals, only 12 were still in place during the last monitoring, indicating 40% mortality. Through photogrammetry, the overall volume change and biomass production were estimated to be $9.24 \pm 5.47\%$ year⁻¹ and 29.52 ± 27.93 g DW year⁻¹, respectively, indicating a general decreasing trend between 2021 and 2023. Signs of necrosis were observed in some individuals, potentially related to the high temperature occurring during summer 2022 and 2023. Considering the current climate crisis, long-term monitoring efforts must be made to better understand the dynamics of this species, and photogrammetry has the potential to be a versatile monitoring tool that will contribute to the standardization of methodologies for sponge growth studies.

Keywords: phenotypic plasticity; Western Mediterranean; sponge ecology; 3D monitoring; climate change



Citation: Pulido Mantas, T.; Roveta, C.; Calcinai, B.; Benelli, F.; Coppari, M.; Di Camillo, C.G.; Pantaleo, U.; Puce, S.; Cerrano, C. Structure from Motion Photogrammetry as an Effective Nondestructive Technique to Monitor Morphological Plasticity in Benthic Organisms: The Case Study of *Sarcotragus foetidus* Schmidt, 1862 (Porifera, Demospongiae) in the Portofino MPA. *Diversity* **2024**, *16*, 175. <https://doi.org/10.3390/d16030175>

Academic Editor: Schiaparelli Stefano

Received: 1 February 2024

Revised: 1 March 2024

Accepted: 4 March 2024

Published: 8 March 2024



Copyright: © 2024 by the authors. Licensee MDPI, Basel, Switzerland. This article is an open access article distributed under the terms and conditions of the Creative Commons Attribution (CC BY) license (<https://creativecommons.org/licenses/by/4.0/>).

1. Introduction

Being sessile filter feeders, Porifera constitute an essential component of marine ecosystems through their role in competitive interactions, bioerosion, benthic–pelagic coupling, carbon flux, and seawater filtration [1–6]. Recently, they have been identified as a precious source of bioactive compounds, as well as an effective model for biotechnological studies and biomonitoring tools for a wide range of pollutants (e.g., trace elements and persistent organic pollutants, among others), e.g., [7,8]. Despite their crucial functional role in marine ecosystems, little is known about the life traits of sponges (e.g., life span, growth rates, and reproductive cycles, among others) [9,10]. The variation in morphology and growth that can occur between locations, populations, or seasons contributes to the

complexity related to this topic [11,12]. Although growth rates have been defined for a few species [1], clear indicators of their annual growth, useful to easily determine rates and age, are still lacking [13].

Estimating sponge growth and biomass traditionally relies on destructive approaches (i.e., wet weight, dry weight, radiocarbon dating methods), e.g., [14,15], often fatal for the organism and not adapted to all sponge growth habits (e.g., encrusting, rope-like, tubular, or massive) [13]. Current methods mainly record two-dimensional (2D) metrics (e.g., planar projection photography), e.g., [9,12,16], even though sponges often present complex three-dimensional (3D) structures [13]. Recently, technological and methodological advancements are helping to develop new techniques to capture 3D features in underwater environments [17]. While earlier 3D imaging methods, such as stereo-photogrammetry, required dual-camera equipment and technical expertise for their implementation [18], the increase in computational power along with the advancements in computer vision algorithms have resulted in the development of Structure from Motion (SfM) photogrammetry, one of the most popular modern procedures [17]. This technique can be applied using a single camera, allowing accurate 3D digital reconstructions from a series of overlapping images [13].

In coralligenous assemblages, one of the most important habitats of the Mediterranean Sea [19], Porifera are among the dominant sessile organisms, with species presenting a variety of growth forms, from erect or massive 3D shapes to encrusting and boring species [20]. In past decades, Mediterranean sponges have followed the fate of many other sessile organisms (e.g., gorgonians, bryozoans, crustose coralline algae), suffering repeated mass mortality events, especially involving those species with a massive shape [21–23]. *Sarcotragus foetidus* Schmidt, 1862 (Demospongiae, Dictyoceratida, Irciinidae), is an irregularly massive sponge with a skeleton made of spongin fibers embedded with sandy debris. *S. foetidus* is considered one of the main ecosystem engineers of coralligenous habitats thanks to its structural complexity and the wide aquiferous system, which act as a refuge for many organisms (e.g., Annelida, Crustacea, Mollusca) [24–27]. Its major threats have been identified as artisanal fishing activities, which eradicate them from the substrate through entanglement in their gear, and the increase in the frequency of mass mortalities linked to periods of anomalous high temperatures [23,28]. Moreover, the species may be exploited due to its potential for use in biomedical applications [29,30]. For these reasons, the species is listed in Annex II of the SPA/BD Protocol of the Barcelona Convention [31].

To the best of our knowledge, no information regarding the growth patterns of this species is currently present in the literature. Thus, the main aim of the current study was to test the feasibility of an innovative technique known as SfM-photogrammetry to assess the growth (volume and biomass production), changes in shape, and eventual disease progression of wild individuals of *S. foetidus* in the Portofino Marine Protected Area (MPA). The development of 3D cost-effective approaches to monitor sponge growth, morphological changes, and the effect of disease/stressors represents a step forward in the monitoring of sessile organisms, making photogrammetry a powerful tool in the implementation of tailored conservation measures and species-based management plans.

2. Materials and Methods

2.1. Study Area, Image Acquisition, and Photogrammetric Processing

The monitored individuals of *S. foetidus* are located on the same boulder at Punta del Faro, Portofino MPA (North-Western Mediterranean [32]) (Figure 1a). From an oceanographic perspective, this area is affected mainly by the Ligurian current, which, together with the narrow continental shelf, produces a highly hydrodynamic tunnel effect in the coast moving from east to west [33]. All individuals surveyed were detected on a wide rock, covering a depth range between 15 and 27 m, where in the past, only a facies of the macroalgae *Ericaria zosteroides* (C. Agardh) Molinari & Guiry 2020 was present and disappeared after the 1999 and 2003 thermal anomalies [22]. Considering the simultaneous appearance of sponges, noticed for the first time in 2014, it is considered that they came

from the same recruitment episode; therefore, they are all approximately the same age (Figure 1b,c).

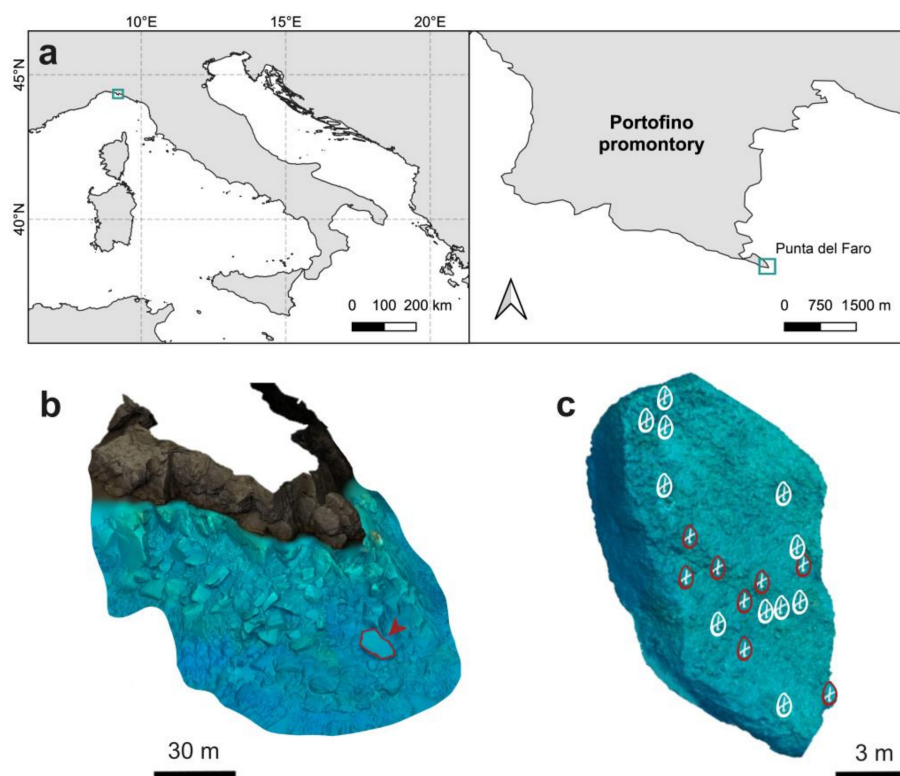


Figure 1. (a) Map indicating the location of Punta del Faro (Portofino MPA, Italy). (b) Three-dimensional reconstruction of the submerged part of the area of interest. The boulder where the *Sarcotragus foetidus* population was monitored is outlined in red and indicated by a red arrow. (c) Details of the surveyed boulder and the exact location of each sponge individual marked with a white “X”. Sponges considered for the volume change analysis are circled in white, while individuals affected by mortality are circled in red.

Sampling activities were carried out in September 2017 (t_1), November 2021 (t_2), and October 2023 (t_3). A GoPro Hero 4 Silver equipped with a 12 Mpixel CMOS f2.8 lens, underwater housing, and an artificial lighting system composed of two 25W Polar Pros was used for the t_1 photographic sampling. Meanwhile, a Sony RX100 V camera system equipped with a ZEISS® Vario-Sonnar T* f/1.8–2.8 24–70 mm lens, underwater housing, and an artificial lighting system composed of two Akkin 5000s was used for the t_2 and t_3 photographic sampling. The photographic protocol consisted of (i) the placement of metric references close to the surveyed sponge individuals and (ii) the capture of a series of overlapping images (40 to 60 pictures). Images were taken around each sponge at an approximate distance of 0.5 m, covering any possible perspective and ensuring a minimum of 60% overlap among consecutive images [34].

To produce the digital reconstructions from the collected images, the software Agisoft Metashape v. 1.8.2. (Agisoft LLC, St. Petersburg, Russia) was used. Camera calibration was implemented automatically as part of the Metashape workflow. First, a set of images was aligned using high-accuracy generic pair selection settings to produce point clouds, limiting the key point limit identification per megapixel to 4000 common features and the tie point limit to 1000. From the sparse cloud, a dense point cloud was obtained, and a mesh was produced with an arbitrary 3D surface type from the dense cloud data, a high face count, and interpolation disabled. To scale up the 3D reconstructions, the deployed metric references were manually detected in the imagery dataset and used to create scale bars in the reference settings.

The overall photogrammetric process to generate, clean, and measure each 3D reconstruction took around 30 min of processing time per sample and sampling time step, using a Lenovo Legion laptop (Beijing, China) with an Intel Core i7-9750H 2.60-GHz processor (Intel Corporation, Santa Clara, CA, USA), 32 Gb RAM, and an NVIDIA GeForce RTX 2060 graphic card (NVIDIA Corporation, Santa Clara, CA, USA).

2.2. Volume and Biomass Estimations

To estimate the volume of each *S. foetidus*, any elements not constituting the surveyed sponge present in the 3D reconstructions (i.e., substrate, metric references, or other benthic organisms) were removed. Subsequently, by using the “close holes” tool inside the mesh toolbox of Agisoft Metashape, the mesh was closed and the volume of each sponge calculated.

To estimate the biomass changes in each individual monitored using SfM-photogrammetry, only in t_1 , samples of other *S. foetidus* ($n = 13$) of similar size were collected in the surrounding area at a similar depth. Samples were weighed and their volume calculated with the water displacement method (i.e., mL of displaced water in a graduated cylinder) [35,36]. Then, samples were dried in an oven at 60 °C for 48 h and weighed a second time to obtain the dry weight (DW) biomass of each sample.

2.3. Analysis of *S. foetidus* Morphological Changes

To assess potential changes in the morphology and shape of the monitored sponges, distance-based mesh comparisons were performed using CloudCompare v2.12 (2022) open-source software. To do so, the models corresponding to the three sampling events (t_1 , t_2 , and t_3) of the same sponge individual were imported into the software; a preliminary manual mesh alignment was performed and finished using the “fine registration” tool, limiting the number of iterations to 99. Once the three model meshes were aligned, using the substrate level as a reference to control the alignment, distances between the t_1 – t_2 and the t_2 – t_3 meshes were calculated by the “Cloud/Mesh Dist” tool.

2.4. Sea Surface Temperature (SST) Data and Marine Heat Wave (MHW) Detection

SST data were collected from the National Oceanic and Atmospheric Administration (NOAA) Optimum Interpolation Sea Surface Temperature (OISST), a product with a global 1/4-degree gridded dataset of Advanced Very High-Resolution Radiometer-derived SSTs at a daily resolution. For MHW detection and description, the SSTs from 1 January 1982 to 31 December 2011 were considered, based on [37,38]. Each MHW was described in terms of intensity, cumulative intensity, duration, frequency, and category (I—moderate, II—strong, III—severe, and IV—extreme) (Table S1) by using the R package *heatwaveR* [39].

2.5. Data Analyses

The volume extracted from the 3D models of *S. foetidus* was expressed in dm^3 . Yearly changes in volume (reported as $\% \text{ year}^{-1}$) were calculated as the difference between the volume of each sponge between t_2 and t_1 , and t_3 and t_2 .

The relationship between the volume and the DW biomass of the collected sponge samples was investigated by performing a regression. Data were tested for normality and homoscedasticity using Shapiro’s and Levene’s tests, respectively. A linear regression was then performed using the stats package in the R software v. 4.3.2 [40], and the obtained equation was used to estimate the biomass of the individuals of *S. foetidus* using the volume calculated from each of the 3D models. Biomass data were expressed in dry weight grams (g DW), and yearly changes in biomass (reported as g DW year^{-1}) were calculated as the difference between the biomass of each sponge between t_2 and t_1 , and t_3 and t_2 .

The experimental design, aiming at testing differences in the volume and biomass changes per year of *S. foetidus* individuals, included one factor: time (random, 2 levels: t_2 – t_1 and t_3 – t_2). Before the analyses, data were tested for normality (Shapiro’s test) and homoscedasticity (Levene’s test); then, a repeated-measures Analysis of Variance (ANOVA)

was performed. Since the yearly biomass data did not meet the assumption of normality, a Friedman test was run.

As for the biomass and volume analyses, also regarding the MHW descriptors, two periods were considered for the analyses: from September 2017 (t_1) to November 2021 (t_2) and from December 2021 to October 2023 (t_3). Differences in the maximum and cumulative intensities, duration, and frequencies of MHWs were investigated between these two periods. Since the data did not meet the assumption of normality, Mann–Whitney tests were performed. Conversely, for the analyses of the SSTs, only the summer periods (from 21st June to 22nd September; Table S2) of each year of monitoring (2018–2023) were considered. Differences among summer SSTs of each year were investigated using the Kruskal–Wallis test, followed by Dunn’s post hoc comparison.

Statistical analyses were carried out using the free software PAST (Paleontological Statistics), version 4.05 [41], considering a 95% confidence level.

3. Results

3.1. SfM-Photogrammetry Assessment

Of the initial 20 individuals of *S. foetidus* surveyed in t_1 , five were not found in t_2 , while three individuals were lost between t_2 and t_3 , indicating a total mortality of 40% in the six years. Among the 12 remaining individuals, two were not included in the volume/biomass analyses due to their high levels of epibiosis, preventing an accurate biometric estimation. Therefore, the final analyses were conducted on a total of 10 sponge individuals (Figure S1).

The 30 digital reconstructions (Figure 2 and Figure S1) produced for the three time steps (t_1 , t_2 , and t_3) had a minimum of 10,011 vertices and 20,012 faces, and averages (\pm SD) of $151,384 \pm 182,162$ vertices and $302,505 \pm 364,008$ faces after the substrate-cleaning process. The reconstructions’ averaged scale error was 0.14 ± 0.09 cm, never exceeding an error of 3 mm. The total time invested in the photogrammetric and cleaning process of all models was around 900 min.

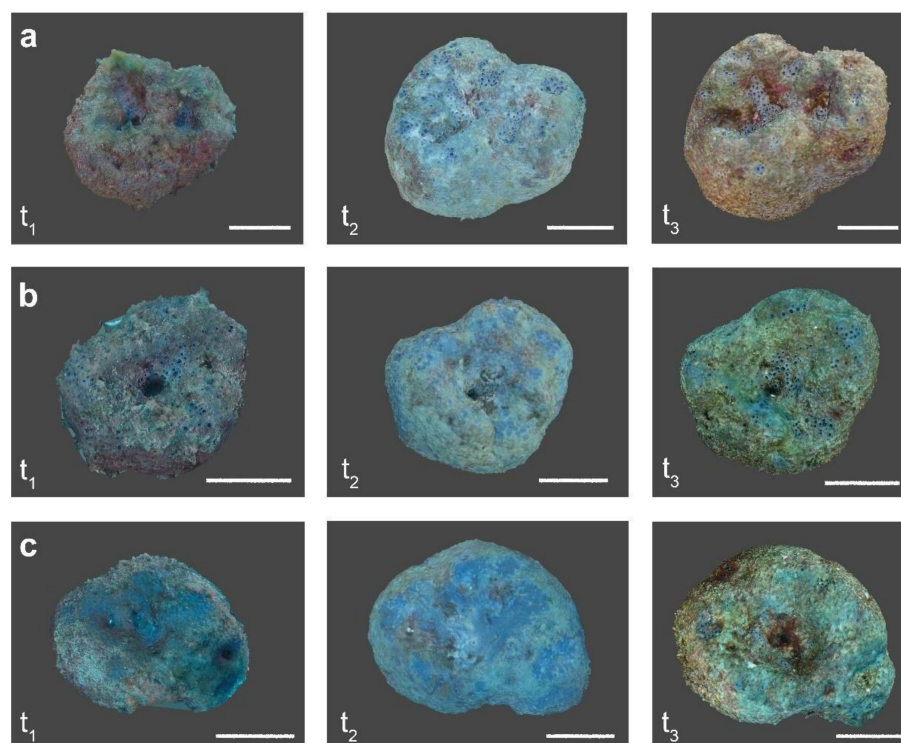


Figure 2. (a–c) Examples of the 3D reconstructions produced for three *Sarcotragus foetidus* individuals over three monitoring time steps (September 2017, t_1 ; November 2021, t_2 ; and October 2023, t_3). Scale bars = 10 cm.

Most of the *S. foetidus* individuals surveyed for this 6-year period displayed a general growth pattern, increasing in height and width in their periphery, while characteristic central aquiferous depression of this sponge species was accentuated (Figures 2 and 3). This polarized growth towards the peripheral upper parts of the sponge is especially evident for the t_1 – t_2 period, where the maximum distances between 3D reconstructions were obtained, reaching an average maximum linear growth of 3.69 ± 1.12 cm. Conversely, in the t_2 – t_3 period, this polarized growth is not so evident, presenting a smaller average maximum linear growth (2.81 ± 1.09 cm). Additionally, the curves of the distributions of the distance values calculated for each 3D comparison show a clearly skewed distribution towards positive distance values for most of the comparisons calculated for the t_1 – t_2 period, highlighting overall positive linear growth (Figure 3 and Figure S1). In contrast, the same curves for the t_2 – t_3 period present a more centered distribution, depicting less marked sponge growth, with most of the distance values close to 0 cm and a higher count of negative distance values (Figure 3 and Figure S1).

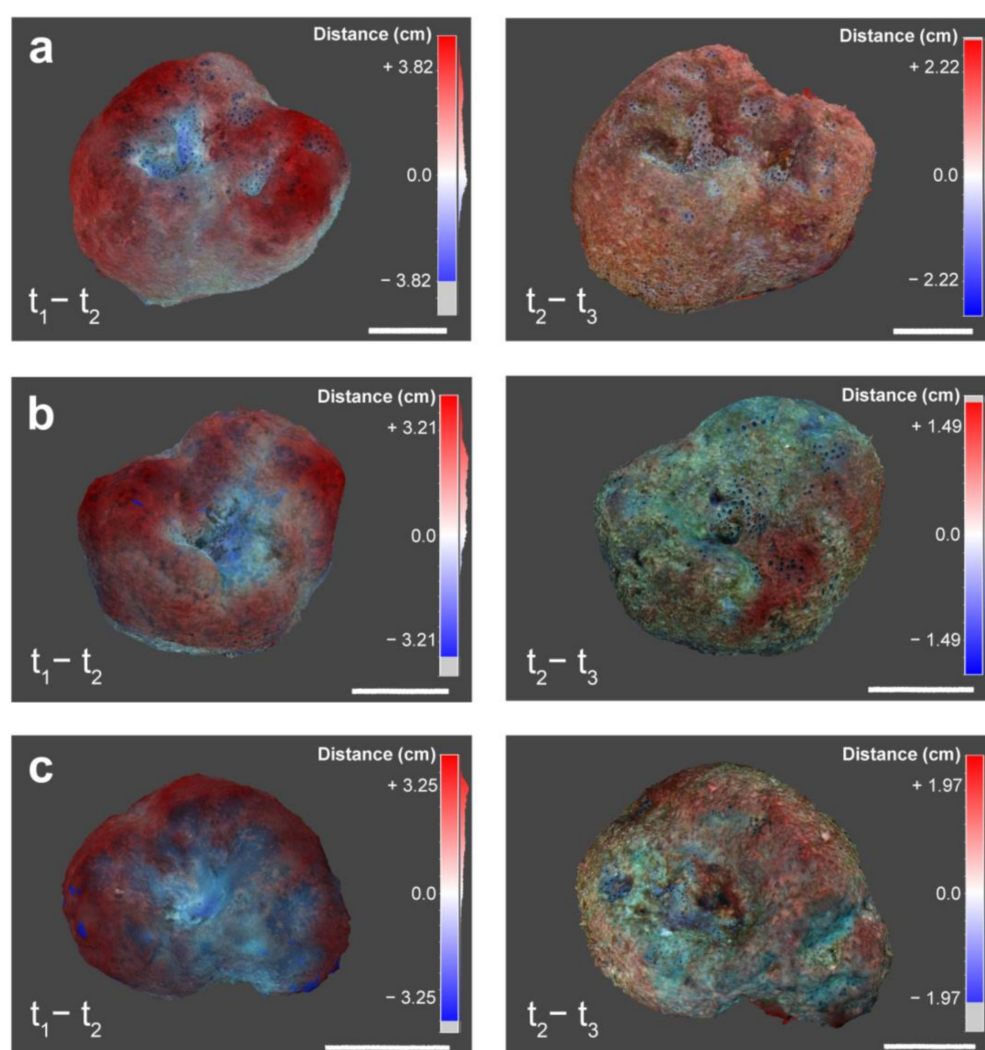


Figure 3. (a–c) Distances calculated between the 3D models of *Sarcotragus foetidus* obtained for t_1 – t_2 (September 2017–November 2021) on the left and t_2 – t_3 (November 2021–October 2023) on the right. Comparisons calculated using point cloud distances in Cloud Compare. Scale bars = 10 cm.

There was a case of an individual of *S. foetidus* affected by necrosis between t_2 and t_3 , which suffered a steep decrease of -3.42% in volume, after a previously regular polarized growth phase during the first considered time period, t_1 – t_2 (Figures 4a and S1c). There were also cases of high epibiotic coverage, such as the brown algae *Padina pavonica*

(Linnaeus) Thivy 1960, preventing accurate volume change estimations for some individuals (Figure 4b).

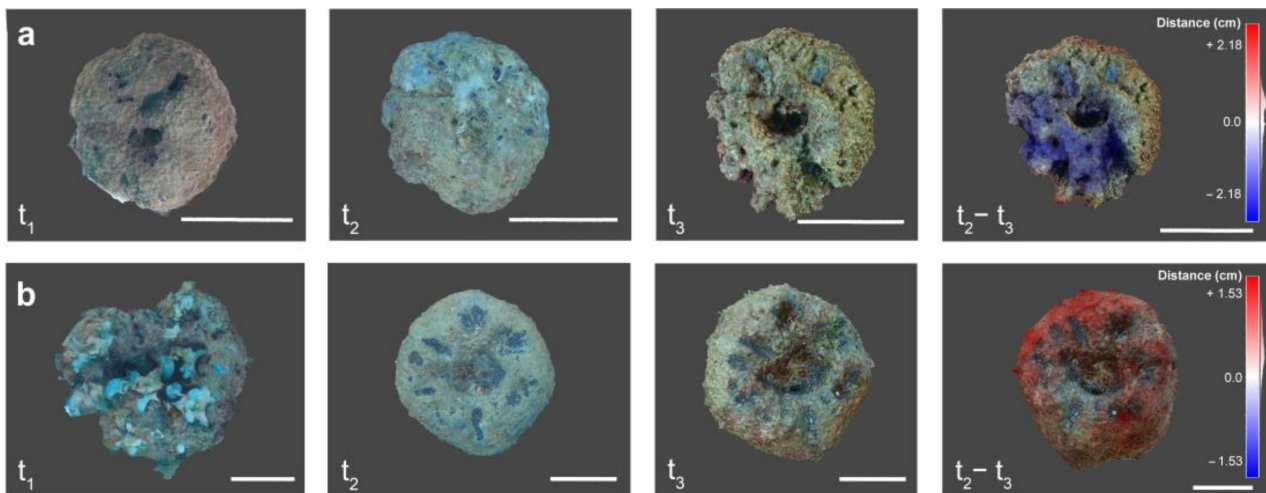


Figure 4. Particular cases regarding the 3D assessment of *Sarcotragus foetidus* changes during this study. (a) *S. foetidus* individual affected by necrosis during the t_2 – t_3 (November 2021–October 2023) period; (b) *S. foetidus* individual affected by a high level of epibiosis by *Padina pavonica*, preventing an accurate t_1 – t_2 (September 2017–November 2021) 3D change assessment. Scale bars = 10 cm.

3.2. Volume and Biomass Changes over Time

The average change in volume of the surveyed *S. foetidus* individuals for the whole monitored period corresponded to an increase of $9.24 \pm 5.47\% \text{ year}^{-1}$. However, by considering the two monitoring periods separately, a significant decline in sponge volume production in t_2 – t_3 was recorded (repeated-measures ANOVA: $df = 1$, $F = 8.827$, p -value = 0.01568), with an average volume increase of $11.95 \pm 5.81\% \cdot \text{year}^{-1}$ in t_1 – t_2 and only $2.34 \pm 8.21\% \cdot \text{year}^{-1}$ in t_2 – t_3 (Figure 5a).

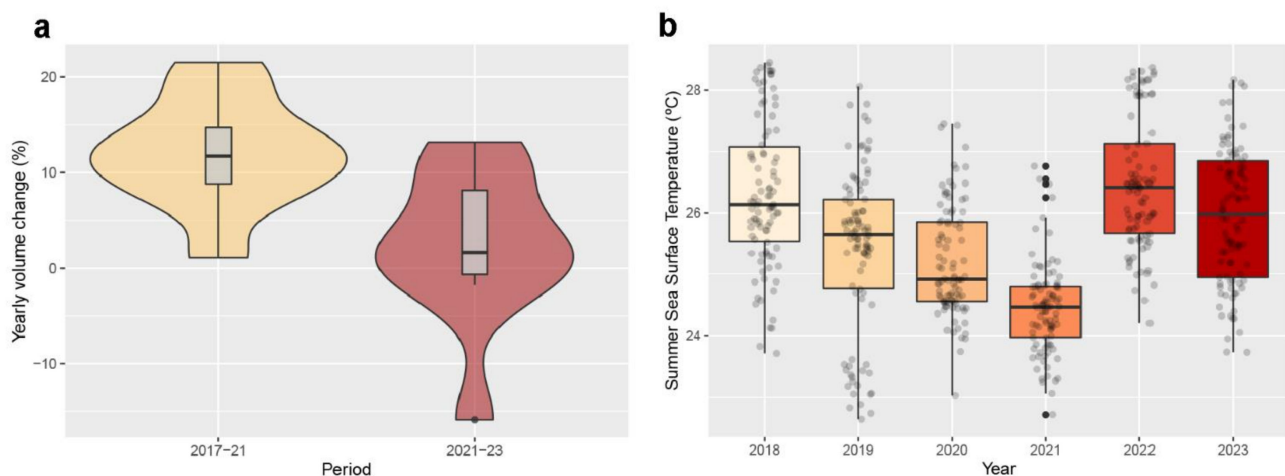


Figure 5. (a) *Sarcotragus foetidus* estimated yearly volume changes (%) for the two periods of this study: t_1 – t_2 (September 2017–November 2021) and t_2 – t_3 (November 2021–October 2023). (b) Boxplots depicting the sea surface temperatures (SSTs) recorded in the Portofino MPA during the summer periods (from 21 June to 22 September) of each monitoring year; the jittered points represent the underlying distribution of the SST data.

The linear regression performed to study the relationship between the volume (x) and the DW biomass (y) found a strong positive correlation ($y = 0.091x + 0.1345$), with a regression coefficient (R^2) of 0.8262 (Figure S2). Using the volumes obtained from the

photogrammetric assessment, an average of 29.52 ± 27.93 g DW · year⁻¹ of biomass production was estimated for the 6 years. However, similarly to the volume, a significant difference in the DW biomass was highlighted between the two periods (Friedman: df = 1, p value = 0.014621), with an estimated biomass production of 37.64 ± 26.01 g DW · year⁻¹ and 2.18 ± 43.47 g DW · year⁻¹ for the t_1 – t_2 and t_2 – t_3 periods, respectively.

3.3. Temperature Analyses

To explore a possible relationship between the drastic drop in sponge growth and the occurrence of anomalous temperatures, the occurrence of MHWs in the area was investigated. Between September 2017 and September 2023, a total of 28 MHWs were identified in the area, with most of the events categorized as I—moderate (17) and II—strong (10), and only one event categorized as III—severe in 2018 (Table S1; Figure S3). Even though no differences were detected in the MHW descriptors (maximum intensity, cumulative intensity, duration, and frequencies) among the two monitoring periods (Mann–Whitney, $p > 0.05$), significant differences were found among the summer-period SSTs of each of the monitoring years (Kruskal–Wallis, $p < 0.001$), with the SSTs registered in 2022 (26.47 ± 1.07 °C), 2018 (26.31 ± 1.20 °C), and 2023 (25.95 ± 1.12 °C) being significantly higher than all other years (Dunn’s post hoc, $p < 0.001$) (Figure 5b).

4. Discussion

Sponges are well represented in the Mediterranean Sea, reaching their highest diversity in coralligenous and marine cave assemblages [19,20,42]. Although taxonomic assessments of the sponge communities in the Portofino MPA have been conducted since the 1990s [43,44], little is known about the conservation status and distribution of a wide range of these species [45]. In this context, the presence of a small population of *S. foetidus*, likely all arising from the same recruitment event, and therefore considered of the same age, provided a unique opportunity to (i) evaluate fine-scale changes at the individual level over time and (ii) observe negative effects potentially related to the unfolding of the current climate crisis.

Although sponge monitoring using photogrammetry is not new, great improvements in terms of technique accuracy and accessibility have been made over the past years [17]. From its early applications using stereo-vision systems [18,46] to the recent SfM-based approaches assessing sponge distributions [47,48], age and growth [13,49,50], or interactions with other organisms [51], photogrammetry has proven its versatility. Our study confirmed once again the suitability of this nondestructive cost-effective technique to survey changes in sponge species, showing how *S. foetidus* exhibited a growth pattern polarized towards the upper peripheral parts of the individual. By comparing sequential 3D reconstructions, it was possible to observe a certain degree of plasticity putatively related to the differential accumulation of sediment in the sponge body. Even if simple-massive sponges are known to be best suited to mid-range environmental conditions [52], *S. foetidus* can live in areas characterized by a high degree of sedimentation [53]. Similar to other species belonging to the family Irciniidae (i.e., *Ircinia* spp.), *S. foetidus* might also take advantage of this high sediment load by using and accumulating it in different parts of its body. In most cases, the typical cushion shape of *S. foetidus* leads to an accumulation of sediment in the central part, triggering the formation of a concave depression that becomes accentuated through time, and eventually leading to the formation of a complete cavity. The final process, not yet documented in the present time-series, leads to specimens with a ring shape, that, with continued growth, will achieve a half-ring shape (Figure 6).

To date, the only previous study assessing the biomass of *S. foetidus* [53] obtained a linear correlation between the sponge size and its DW. Analogously, the current study found a similarly strong linear correlation between a sponge’s volume and its DW. In addition, *S. foetidus*’ growth rate was estimated for the first time, previously only known for the congeners *Sarcotragus spinosulus* Schmidt, 1862 (100% year⁻¹), and *Sarcotragus fasciculatus* (Pallas, 1766) ($40.03 \pm 4.81\%$ year⁻¹) [54,55], both showing higher rates of volume increase

compared to our results ($9.24 \pm 5.47\%$ year⁻¹). As already stated, these strong differences might be related to various factors, such as the species-specific growth rate, the different ages of the surveyed organisms [13,56], or the fact that the surveyed organisms were under increasing stress conditions due to the recurrent episodes of thermal anomalies in the area.

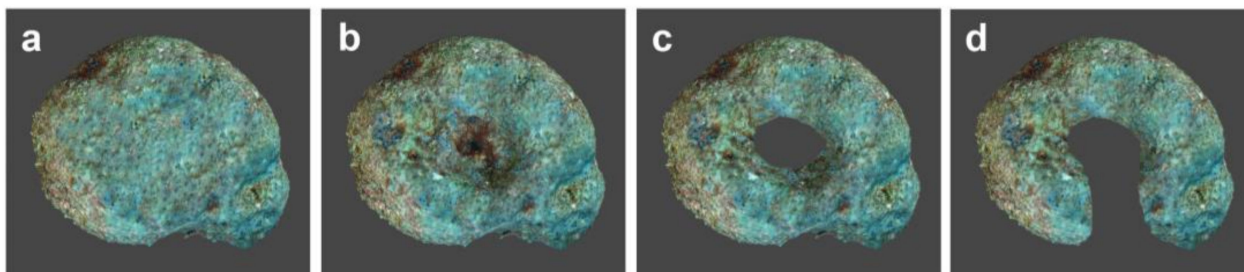


Figure 6. Growth phases of *Sarcotragus foetidus*: (a) initial growth phase of a cushion-shaped specimen; (b) specimen where sediments accumulating in the center of the sponge trigger reshaping through a central depression; (c) with the enlargement of the cavity, sediments are released on the sea floor and the sponge takes on a ring shape; (d) the continuous growth of the sponge leads to a perforated horseshoe shape. Although observed in several other areas, (c,d) are virtually reconstructed images of the potential development of the monitored individuals.

In the context of an ever-warmer Mediterranean, gradual shifts in shallow benthic communities are expected towards a dominance of thermo-tolerant species [57]. Even though some sponges are able to cope with short-term thermal-stress conditions [58], *S. foetidus* has been reported to be a thermo-sensitive species, showing mortalities up to 9% and estimations of necrotized individuals up to 27% during a mass mortality event recorded in the summer of 2021 [59]. Dinçtürk et al. [59] reported two main causes triggering species mortality in the Aegean Sea: elevated SSTs for a long-term period (i.e., several months) and the proliferation of different pathogenic *Vibrio* species, which aggravated the health status of the already stressed sponges. In our case, of the initial 20 individuals surveyed, 25% were lost between September 2017 and November 2021, potentially as a consequence of the synergy of the high average temperatures in summer and the exceptional storm that occurred in October 2018, whose devastating effects were evident up to a depth of 25 m [60]. A total of 20% of the remaining *S. foetidus* were instead lost between 2021 and 2023, potentially related to the average summer temperatures of 2022 (26.47 ± 1.07 °C) and 2023 (26.31 ± 1.20 °C), significantly higher than all other analyzed years. The effect of climate change was also evident in individuals still in place during the last monitoring but showing necrotic portions (see Figure 4a). Episodes of extensive necrosis of keratose sponges have been documented in the Mediterranean Sea in recent decades [23,28,59,61]. In addition, recurrent mortality events of *Cacospongia* spp., *Ircinia* spp. and *Spongia* spp., *Petrosia* (*Petrosia*) *ficiformis* (Poiret, 1789), and *Agelas oroides* (Schmidt, 1864) (unpublished data) have been observed in the study area. Additional mid-term and long-term monitoring efforts must be made to better understand the population dynamics of this species under the current climate crisis [59].

The application of SfM-photogrammetry has enabled us to achieve a step forward in biological sciences, allowing us to perceive processes from a more complete and realistic perspective [3,62]. In terms of sponge assessments, its systematic application could constitute a versatile monitoring tool for many different species and morphotypes, contributing to the harmonization of methodologies and units for growth studies. This would increase the comparability of growth studies, a recurrent issue found in the literature. Additionally, the increasing access to low-cost, high-resolution underwater camera equipment [63], together with the rise of citizen science initiatives, could play a fundamental role by reducing monitoring costs, supporting scientific research efforts in the assessment of our precious and impacted underwater environments, and ultimately, raising awareness in the local community about the rapid changes occurring in marine communities [64].

Supplementary Materials: The following supporting information can be downloaded at: <https://www.mdpi.com/article/10.3390/d16030175/s1>, Table S1: Marine heat wave (MHW) metrics obtained for the identified MHWs inside the Portofino MPA during the years considered in this study. Table S2: Sea surface temperatures (SSTs) recorded in Portofino (Liguria, Italy) from September 2017 to November 2023; Figure S1: *Sarcotragus foetidus* 3D reconstructions produced (2017, 2021, and 2023) and 3D Comparisons calculated using point cloud distances in Cloud Compare. Scale bars = 10 cm. Figure S2: Linear regression calculated for the study of volume–biomass relationships. Figure S3: Maximum intensity of the marine heat waves that occurred at the Portofino MPA from September 2015 to November 2023.

Author Contributions: Conceptualization, methodology, and supervision, C.C. and U.P.; fieldwork, F.B., T.P.M. and C.R.; formal analysis, investigation, and data curation, F.B., C.R., M.C. and T.P.M.; writing—original draft preparation, F.B., C.R., M.C. and T.P.M.; writing—review and editing, C.C., C.R., F.B., B.C., M.C., C.G.D.C., S.P., U.P. and T.P.M.; visualization, F.B., U.P., C.G.D.C., B.C., S.P. and T.P.M. All authors have read and agreed to the published version of the manuscript.

Funding: The current project was funded under the National Recovery and Resilience Plan (NRRP), Mission 4, Component 2, Investment 1.4—Call for tender No. 3138 of 16 December 2021, rectified by Decree n.3175 of 18 December 2021, of the Italian Ministry of University and Research funded by the European Union—NextGenerationEU; Award Number: Project code CN_00000033, Concession Decree No. 1034 of 17 June 2022 adopted by the Italian Ministry of University and Research, CUP D33C22000960007, Project title “National Biodiversity Future Center—NBFC”. This project was also partially funded by the Interreg Med MPA Engage “Engaging Mediterranean key actors in Ecosystem Approach to manage Marine Protected Areas to face Climate change” (grant number 5216).

Institutional Review Board Statement: Not applicable.

Data Availability Statement: All relevant data are presented within the manuscript and the provided Supplementary Materials.

Acknowledgments: The authors are thankful to the staff of the Portofino Marine Protected Area, and to Portofino Divers and Style Diving for the logistic support during diving activities partially performed in the framework of the MP-Engage project. The authors are also thankful to the Reef Alert Network and for the invaluable work of the volunteers Jenny Kunze, Peter Knessl, Sabrina Koslowski, and Giorgia Sanna, who helped during the photogrammetric sampling in the framework of the Conservation Diver Course (<https://portofinodivers.com/en/marine-conservation-volunteering.html>) (accessed on 6 March 2024). The authors wish to also thank Daniel Cossey for having dedicated his time to the proof reading of the final manuscript.

Conflicts of Interest: The authors declare that this research was conducted in the absence of any commercial or financial relationships that could be construed as potential conflicts of interest.

References

1. Bell, J.J. The functional roles of marine sponges. *Estuar. Coast. Shelf Sci.* **2008**, *79*, 341–353. [[CrossRef](#)]
2. Van Soest, R.W.; Boury-Esnault, N.; Vacelet, J.; Dohrmann, M.; Erpenbeck, D.; De Voogd, N.J.; Santodomingo, N.; Vanhoorne, B.; Kelly, M.; Hooper, J.N. Global diversity of sponges (Porifera). *PLoS ONE* **2012**, *7*, e35105. [[CrossRef](#)] [[PubMed](#)]
3. Maldonado, M.; Aguilar, R.; Bannister, R.; Bell, J.; Conway, J.; Dayton, P.; Díaz, C.; Gutt, J.; Kelly, M.; Kenchington, E.; et al. Sponge Grounds as Key Marine Habitats: A Synthetic Review of Types, Structure, Functional Roles, and Conservation Concerns. In *Marine Animal Forests: The Ecology of Benthic Biodiversity Hotspots*; Rossi, S., Bramanti, L., Gori, A., Orejas, S.d.V.C., Eds.; Springer: Cham, Switzerland, 2017; pp. 1–39. [[CrossRef](#)]
4. Weisz, J.B.; Lindquist, N.; Martens, C.S. Do associated microbial abundances impact marine demosponge pumping rates and tissue densities? *Oecologia* **2008**, *155*, 367–376. [[CrossRef](#)] [[PubMed](#)]
5. Maldonado, M.; Ribes, M.; van Duyl, F.C. Nutrient fluxes through sponges: Biology, budgets, and ecological implications. *Adv. Mar. Biol.* **2012**, *62*, 113–182. [[CrossRef](#)] [[PubMed](#)]
6. Pham, C.K.; Murillo, F.J.; Lirette, C.; Maldonado, M.; Colaço, A.; Ottaviani, D.; Kenchington, E. Removal of deep-sea sponges by bottom trawling in the Flemish Cap area: Conservation, ecology and economic assessment. *Sci. Rep.* **2019**, *9*, 15843. [[CrossRef](#)] [[PubMed](#)]
7. Di Cesare Mannelli, L.; Palma Esposito, F.; Sangiovanni, E.; Pagano, E.; Mannucci, C.; Polini, B.; Ghelardini, C.; Dell’Agli, M.; Izzo, A.A.; Calapai, G.; et al. Pharmacological activities of extracts and compounds isolated from mediterranean sponge sources. *Pharmaceuticals* **2021**, *14*, 1329. [[CrossRef](#)] [[PubMed](#)]

8. Roveta, C.; Annibaldi, A.; Afghan, A.; Calcinai, B.; Di Camillo, C.G.; Gregorin, C.; Illuminati, S.; Pulido Mantas, T.; Truzzi, C.; Puce, S. Biomonitoring of heavy metals: The unexplored role of marine sessile taxa. *Appl. Sci.* **2021**, *11*, 580. [[CrossRef](#)]
9. Garrabou, J.; Zabala, M. Growth dynamics in four Mediterranean demosponges. *Estuar. Coast. Shelf Sci.* **2001**, *52*, 293–303. [[CrossRef](#)]
10. Riesgo, A.; Maldonado, M. Differences in reproductive timing among sponges sharing habitat and thermal regime. *Invertebr. Biol.* **2008**, *127*, 357–367. [[CrossRef](#)]
11. Pronzato, R.; Bavestrello, G.; Cerrano, C. Morpho-functional adaptations of three species of *Spongia* (Porifera, Demospongiae) from a Mediterranean vertical cliff. *Bull. Mar. Sci.* **1998**, *63*, 317–328.
12. Gökalp, M.; Kooistra, T.; Rocha, M.S.; Silva, T.H.; Osinga, R.; Murk, A.J.; Wijgerde, T. The effect of depth on the morphology, bacterial clearance, and respiration of the Mediterranean sponge *Chondrosia reniformis* (Nardo, 1847). *Mar. Drugs* **2020**, *18*, 358. [[CrossRef](#)]
13. Olinger, L.K.; Scott, A.R.; McMurray, S.E.; Pawlik, J.R. Growth estimates of Caribbean reef sponges on a shipwreck using 3D photogrammetry. *Sci. Rep.* **2019**, *9*, 18398. [[CrossRef](#)]
14. Roche, S.; Ronziere, M.C.; Herbage, D.; Freyria, A.M. Native and DPPA cross-linked collagen sponges seeded with fetal bovine epiphyseal chondrocytes used for cartilage tissue engineering. *Biomaterials* **2000**, *22*, 9–18. [[CrossRef](#)]
15. Çelik, İ.; Cirik, Ş.; Altunağaç, U.; Ayaz, A.; Çelik, P.; Tekeşoğlu, H.; Yılmaz, H.; Öztekin, A. Growth performance of bath sponge (*Spongia officinalis* Linnaeus, 1759) farmed on suspended ropes in the Dardanelles (Turkey). *Aquac. Res.* **2011**, *42*, 1807–1815. [[CrossRef](#)]
16. De Caralt, S.; Uriz, M.J.; Wijffels, R.H. Grazing, differential size-class dynamics and survival of the Mediterranean sponge *Corticium candelabrum*. *Mar. Ecol. Prog. Ser.* **2008**, *360*, 97–106. [[CrossRef](#)]
17. Pulido Mantas, T.; Roveta, C.; Calcinai, B.; Di Camillo, C.G.; Gambardella, C.; Gregorin, C.; Coppari, M.; Marrocco, T.; Puce, S.; Riccardi, A.; et al. Photogrammetry, from the Land to the Sea and Beyond: A Unifying Approach to Study Terrestrial and Marine Environments. *J. Mar. Sci. Eng.* **2023**, *11*, 759. [[CrossRef](#)]
18. Koopmans, M.; Wijffels, R.H. Seasonal growth rate of the sponge *Haliclona oculata* (Demospongiae: Haplosclerida). *Mar. Biotechnol.* **2008**, *10*, 502–510. [[CrossRef](#)] [[PubMed](#)]
19. Bevilacqua, S.; Airoidi, L.; Ballesteros, E.; Benedetti-Cecchi, L.; Boero, F.; Bulleri, F.; Cebrian, E.; Cerrano, C.; Claudet, J.; Colloca, F.; et al. Mediterranean rocky reefs in the Anthropocene: Present status and future concerns. *Adv. Mar. Biol.* **2021**, *89*, 1–51. [[CrossRef](#)] [[PubMed](#)]
20. Bertolino, M.; Cerrano, C.; Bavestrello, G.; Carella, M.; Pansini, M.; Calcinai, B. Diversity of Porifera in the Mediterranean coralligenous accretions, with description of a new species. *ZooKeys* **2013**, *336*, 1–37. [[CrossRef](#)] [[PubMed](#)]
21. Di Camillo, C.G.; Cerrano, C. Mass mortality events in the NW Adriatic Sea: Phase shift from slow-to fast-growing organisms. *PLoS ONE* **2015**, *10*, e0126689. [[CrossRef](#)] [[PubMed](#)]
22. Garrabou, J.; Gómez-Gras, D.; Ledoux, J.B.; Linares, C.; Bensoussan, N.; López-Sendino, P.; Bazairi, H.; Espinosa, F.; Ramdani, M.; Grimes, S.; et al. Collaborative database to track mass mortality events in the Mediterranean Sea. *Front. Mar. Sci.* **2019**, *6*, 478167. [[CrossRef](#)]
23. Garrabou, J.; Gómez-Gras, D.; Medrano, A.; Cerrano, C.; Ponti, M.; Schlegel, R.; Bensoussan, N.; Turicchia, E.; Sini, M.; Gerovasileiou, V.; et al. Marine heatwaves drive recurrent mass mortalities in the Mediterranean Sea. *Glob. Change Biol.* **2022**, *28*, 5708–5725. [[CrossRef](#)] [[PubMed](#)]
24. Gerovasileiou, V.; Chintiroglou, C.C.; Konstantinou, D.; Voultsiadou, E. Sponges as “living hotels” in Mediterranean marine caves. *Sci. Mar.* **2016**, *80*, 279–289. [[CrossRef](#)]
25. Pola, L.; Cerrano, C.; Del Sette, G.; Torsani, F.; Calcinai, B. Seasonal trend of the macrofauna inhabiting two Mediterranean species of *Sarcotragus* (Porifera, Demospongiae). In Proceedings of the 53rd European Marine Biology Symposium, Ostend, Belgium, 17–21 September 2018.
26. Çınar, M.E.; Bakir, K.; Doğan, A.; Acik, S.; Kurt, G.; Katağan, T.; Öztürk, B.; Dağlı, E.; Özcan, T.; Kirkim, F.; et al. Macro-benthic invertebrates associated with the black sponge *Sarcotragus foetidus* (Porifera) in the Levantine and Aegean Seas, with special emphasis on alien species. *Estuarine. Coast. Shelf Sci.* **2019**, *227*, 106306. [[CrossRef](#)]
27. Goren, L.; Idan, T.; Shefer, S.; Ilan, M. Macrofauna inhabiting massive demosponges from shallow and mesophotic habitats along the Israeli Mediterranean coast. *Front. Mar. Sci.* **2021**, *7*, 612779. [[CrossRef](#)]
28. Gerovasileiou, V.; Dailianis, T.; Sini, M.; Otero, M.D.M.; Numa, C.; Katsanevakis, S.; Voultsiadou, E. Assessing the regional conservation status of sponges (Porifera): The case of the Aegean ecoregion. *Mediterr. Mar. Sci.* **2018**, *19*, 526–537. [[CrossRef](#)]
29. Chaudhari, S.; Kumar, M.S. Marine sponges *Sarcotragus foetidus*, *Xestospongia carbonaria* and *Spongia obscura* constituents ameliorate IL-1 β and IL-6 in lipopolysaccharide-induced RAW 264.7 macrophages and carrageenan-induced oedema in rats. *Inflammopharmacology* **2020**, *28*, 1091–1119. [[CrossRef](#)] [[PubMed](#)]
30. Pozzolini, M.; Tassara, E.; Doderò, A.; Castellano, M.; Vicini, S.; Ferrando, S.; Aicardi, S.; Cavallo, D.; Bertolino, M.; Petrenko, I.; et al. Potential biomedical applications of collagen filaments derived from the marine demosponges *Ircinia oros* (Schmidt, 1864) and *Sarcotragus foetidus* (Schmidt, 1862). *Mar. Drugs* **2021**, *19*, 563. [[CrossRef](#)]
31. UNEP/MAP-SPA/RAC. SAP/RAC: SPA-BD Protocol—Annex II: List of Endangered or Threatened Species. 2018. Available online: https://www.rac-spa.org/sites/default/files/annex/annex_2_en_20182.pdf (accessed on 6 March 2024).

32. Spalding, M.D.; Fox, H.E.; Allen, G.R.; Davidson, N.; Ferdeña, Z.A.; Finlayson, M.A.X.; Halpern, B.S.; Jorge, M.A.; Lombana, A.; Lourie, S.A.; et al. Marine ecoregions of the world: A bioregionalization of coastal and shelf areas. *BioScience* **2007**, *57*, 573–583. [CrossRef]
33. Manca Zeichen, M.; Finoia, M.G.; Locritani, M.; Ruggeri, N.; Tunesi, L.; Gasparini, G.P.; Bassetti, M.; Grandi, V.; Cattaneo-Vietti, R.; Povero, P. A preliminary analysis of in situ and remotely sensed environmental variables in the coastal region of the Portofino Marine Protected Area. *Chem. Ecol.* **2008**, *24*, 57–66. [CrossRef]
34. Bayley, D.T.; Mogg, A.O. A protocol for the large-scale analysis of reefs using Structure from Motion photogrammetry. *Methods Ecol. Evol.* **2020**, *11*, 1410–1420. [CrossRef]
35. Çınar, M.E.; Katagan, T.; Ergen, Z.; Sezgin, M. Zoobenthos-inhabiting *Sarcotragus muscarum* (Porifera: Demospongiae) from the Aegean Sea. *Hydrobiologia* **2002**, *482*, 107–117. [CrossRef]
36. Özcan, T.; Katakın, T. Decapod Crustaceans associated with the sponge *Sarcotragus muscarum* Schmidt, 1864 (Porifera: Demospongiae) from the Levantine coasts of Turkey. *Iran. J. Fish. Sci.* **2011**, *10*, 286–293.
37. Hobday, A.J.; Alexander, L.V.; Perkins, S.E.; Smale, D.A.; Straub, S.C.; Oliver, E.C.; Benthuyssen, A.; Burrows, M.T.; Donat, M.G.; Feng, M.; et al. A hierarchical approach to defining marine heatwaves. *Prog. Oceanogr.* **2016**, *141*, 227–238. [CrossRef]
38. Hobday, A.J.; Oliver, E.C.J.; Sen Gupta, A.; Benthuyssen, J.A.; Burrows, M.T.; Donat, M.G.; Holbrook, N.J.; Moore, P.J.; Thomsen, M.S.; Wernberg, T.; et al. Categorising and naming marine heatwaves. *Oceanography* **2018**, *31*, 162–173. [CrossRef]
39. Schlegel, R.W.; Smit, A.J. Heatwaver: A central algorithm for the detection of heatwaves and cold-spells. *J. Open Source Softw.* **2018**, *3*, 821. [CrossRef]
40. R Core Team. *R: A Language and Environment for Statistical Computing*; Foundation for Statistical Computing: Vienna, Austria, 2023; Available online: <https://www.R-project.org/> (accessed on 6 March 2024).
41. Hammer, Ø.; Harper, D.A.T.; Ryan, P.D. PAST: Paleontological statistics software package for education and data analysis. *Palaeontol. Electron.* **2001**, *4*, 1–9.
42. Gerovasileiou, V.; Voultziadou, E. Marine caves of the Mediterranean Sea: A sponge biodiversity reservoir within a biodiversity hotspot. *PLoS ONE* **2012**, *7*, e39873. [CrossRef] [PubMed]
43. Pansini, M. *Petrosia pulitzeri* n. sp. (Porifera, Demospongiae) from Mediterranean caves. *Ital. J. Zool.* **1996**, *63*, 169–172. [CrossRef]
44. Bertolino, M.; Calcinaï, B.; Cattaneo-Vietti, R.; Cerrano, C.; Lafratta, A.; Pansini, M.; Pica, D.; Bavestrello, G. Stability of the sponge assemblage of Mediterranean coralligenous concretions along a millennial time span. *Mar. Ecol.* **2014**, *35*, 149–158. [CrossRef]
45. Azzola, A.; Bavestrello, G.; Bertolino, M.; Bianchi, C.N.; Bo, M.; Enrichetti, F.; Morri, C.; Oprandi, A.; Toma, M.; Montefalcone, M. You cannot conserve a species that has not been found: The case of the marine sponge *Axinella polypoides* in Liguria, Italy. *Aquat. Conserv. Mar. Freshw. Ecosyst.* **2021**, *31*, 737–747. [CrossRef]
46. Abdo, D.A.; Seager, J.W.; Harvey, E.S.; McDonald, J.I.; Kendrick, G.A.; Shortis, M.R. Efficiently measuring complex sessile epibenthic organisms using a novel photogrammetric technique. *J. Exp. Mar. Biol. Ecol.* **2006**, *339*, 120–133. [CrossRef]
47. Rodríguez-Basalo, A.; Prado, E.; Sánchez, F.; Ríos, P.; Gómez-Ballesteros, M.; Cristobo, J. High resolution spatial distribution for the hexactinellid sponges *Asconema setubalense* and *Pheronema carpenteri* in the Central Cantabrian Sea. *Front. Mar. Sci.* **2021**, *8*, 612761. [CrossRef]
48. Ríos, P.; Prado, E.; Carvalho, F.C.; Sánchez, F.; Rodríguez-Basalo, A.; Xavier, J.R.; Ibarrola, T.P.; Cristobo, J. Community composition and habitat characterization of a rock sponge aggregation (Porifera, Corallistidae) in the Cantabrian Sea. *Front. Mar. Sci.* **2020**, *7*, 578. [CrossRef]
49. Prado, E.; Cristobo, J.; Rodríguez-Basalo, A.; Ríos, P.; Rodríguez-Cabello, C.; Sánchez, F. In situ growth rate assessment of the hexactinellid sponge *Asconema setubalense* using 3D photogrammetric reconstruction. *Front. Mar. Sci.* **2021**, *8*, 26. [CrossRef]
50. Idan, T.; Goren, L.; Shefer, S.; Ilan, M. Sponges in a changing climate: Survival of *Agelas oroides* in a warming Mediterranean Sea. *Front. Mar. Sci.* **2020**, *7*, 603593. [CrossRef]
51. Olinger, L.K.; Chaves-Fonnegra, A.; Enochs, I.C.; Brandt, M.E. Three competitors in three dimensions: Photogrammetry reveals rapid overgrowth of coral during multispecies competition with sponges and algae. *Mar. Ecol. Prog. Ser.* **2021**, *657*, 109–121. [CrossRef]
52. Schönberg, C.H.L. No taxonomy needed: Sponge functional morphologies inform about environmental conditions. *Ecol. Indic.* **2021**, *129*, 107806. [CrossRef]
53. Enrichetti, F.; Bavestrello, G.; Betti, F.; Coppari, M.; Toma, M.; Pronzato, R.; Canese, S.; Bertolino, M.; Costa, G.; Pansini, M.; et al. Keratose-dominated sponge grounds from temperate mesophotic ecosystems (NW Mediterranean Sea). *Mar. Ecol.* **2020**, *41*, e12620. [CrossRef]
54. Turon, X.; Garriga, A.; Erwin, P.M. Lights and shadows: Growth patterns in three sympatric and congeneric sponges (*Ircinia* spp.) with contrasting abundances of photosymbionts. *Mar. Biol.* **2013**, *160*, 2743–2754. [CrossRef]
55. Perez-Lopez, P.; Ledda, F.D.; Bisio, A.; Feijoo, G.; Perino, E.; Pronzato, R.; Manconi, R.; Moreira, M.T. Life cycle assessment of in situ mariculture in the Mediterranean Sea for the production of bioactive compounds from the sponge *Sarcotragus spinosulus*. *J. Clean. Prod.* **2017**, *142*, 4356–4368. [CrossRef]
56. Garate, L.; Blanquer, A.; Uriz, M.J. Contrasting biological features in morphologically cryptic Mediterranean sponges. *PeerJ* **2017**, *5*, e3490. [CrossRef]
57. Webster, N.; Pantile, R.; Botte, E.; Abdo, D.; Andreakis, N.; Whalan, S. A complex life cycle in a warming planet: Gene expression in thermally stressed sponges. *Mol. Ecol.* **2013**, *22*, 1854–1868. [CrossRef] [PubMed]

58. Koutsouveli, V.; Manousaki, T.; Riesgo, A.; Lagnel, J.; Kollias, S.; Tsigenopoulos, C.S.; Arvanitidis, C.; Dounas, C.; Magoulas, A.; Dailianis, T. Gearing up for warmer times: Transcriptomic response of risk of mortality outbreaks associated with thermal stress in NW Mediterranean coastal areas. *Ocean Dyn.* **2020**, *64*, 103–115. [[CrossRef](#)]
59. Dinçtürk, E.; Öndes, F.; Leria, L.; Maldonado, M. Mass mortality of the keratose sponge *Sarcotragus foetidus* in the Aegean Sea (Eastern Mediterranean) correlates with proliferation of *Vibrio* bacteria in the tissues. *Front. Microbiol.* **2023**, *14*, 1272733. [[CrossRef](#)] [[PubMed](#)]
60. Betti, F.; Bavestrello, G.; Bo, M.; Enrichetti, F.; Cattaneo-Viatti, R. Effects of the 2018 exceptional storm on the *Paramuricea clavata* (Anthozoa, Octocorallia) population of the Portofino Promontory (Mediterranean Sea). *Reg. Stud. Mar. Sci.* **2020**, *34*, 101037. [[CrossRef](#)]
61. Cebrian, E.; Uriz, M.J.; Garrabou, J.; Ballesteros, E. Sponge mass mortalities in a warming Mediterranean Sea: Are cyanobacteria-harboring species worse off? *PLoS ONE* **2011**, *6*, e20211. [[CrossRef](#)] [[PubMed](#)]
62. Ferrari, R.; Lachs, L.; Pygas, D.R.; Humanes, A.; Sommer, B.; Figueira, W.F.; Edwards, A.J.; Bythell, J.C.; Guest, J.R. Photogrammetry as a tool to improve ecosystem restoration. *Trends Ecol. Evol.* **2021**, *36*, 1093–1101. [[CrossRef](#)]
63. Raoult, V.; David, P.A.; Dupont, S.F.; Mathewson, C.P.; O'Neill, S.J.; Powell, N.N.; Williamson, J.E. GoPros™ as an underwater photogrammetry tool for citizen science. *PeerJ* **2016**, *4*, e1960. [[CrossRef](#)]
64. Garrabou, J.; Bensoussan, N.; di Franco, A.; Boada, J.; Cebrian, E.; Santamaria, J.; Guala, I.; Grech, D.; Cerrano, C.; Pulido Mantas, T.; et al. *Monitoring Climate-Related Responses in Mediterranean Marine Protected Areas and Beyond: Eleven Standard Protocols*; Institute of Marine Sciences, Spanish Research Council ICM-CSIC: Barcelona, Spain, 2022; 74p. [[CrossRef](#)]

Disclaimer/Publisher's Note: The statements, opinions and data contained in all publications are solely those of the individual author(s) and contributor(s) and not of MDPI and/or the editor(s). MDPI and/or the editor(s) disclaim responsibility for any injury to people or property resulting from any ideas, methods, instructions or products referred to in the content.